

Clinical Feasibility of Gadoteric Acid–Enhanced Isotropic High-Resolution 3-Dimensional Magnetic Resonance Cholangiography Using an Iterative Denoising Algorithm for Evaluation of the Biliary Anatomy of Living Liver Donors

Hyo-Jin Kang, MD,*† Jeong Min Lee, MD,*† Su Joa Ahn, MD,‡ Jae Seok Bae, MD,*†
Stephan Kannengiesser, PhD,§ Berthold Kiefer, PhD,§ and Kyung-Suk Suh, MD||

Objectives: The aim of this study was to evaluate the clinical feasibility of gadoteric acid–enhanced isotropic high-resolution (IHR) 3-dimensional (3D) T1-weighted (T1W) magnetic resonance cholangiography (MRC) using an iterative denoising (ID) algorithm for evaluation of the biliary anatomy of living liver donors in comparison with conventional 3D multislice T2-weighted (T2W) MRC.

Materials and Methods: In this institutional review board–approved retrospective study, a total of 75 living liver donors who underwent conventional 3D multislice T2W-MRC and IHR-3D-T1W-MRC on a 3 T scanner and subsequent right hepatectomy for liver donation were included. Isotropic high-resolution T1W-MRCs were obtained in both axial and coronal planes using the 3D VIBE Dixon sequence and an ID algorithm implemented with wavelet thresholding of 3D complex-valued data of the noise level, g-factor, and k-space filtering. Thereafter, 3 board-certified radiologists independently reviewed the examinations for visibility and sharpness of the bile ducts (BDs), as well as overall image quality on a 5-point scale. For diagnostic performance, anatomic variations of the BD, length of right hepatic duct, and the expected number of BD openings at right hepatectomy were also recorded. As the reference standard, BD variation was determined by surgeons in consensus using intraoperative real-time fluorescent cholangiography. **Results:** Mean acquisition times of 3D-T2W-MRC and IHR-T1W-MRC were 367 seconds and 17 seconds ($P < 0.001$), respectively. Compared with 3D-T2W-MRCs, IHR-T1W-MRCs yielded significantly improved visibility and sharpness of all evaluated intrahepatic bile ducts (all P s < 0.05), and higher overall image quality ($P < 0.01$). The IHR-T1W-MRCs also demonstrated significantly higher agreement in BD variation (87.6% vs 81.3%, $P = 0.03$) and expected BD openings (76.9% vs 70.2%, $P = 0.006$) than 3D-T2W-MRC compared with the reference standard. Interobserver agreement in estimating the length of right hepatic duct, IHR-T1W-MRC showed excellent interobserver agreement (intraclass correlation coefficient, 0.94), whereas 3D-T2W-MRC showed good interobserver agreement (intraclass correlation coefficient, 0.78).

Conclusions: Isotropic high-resolution T1W-MRCs with ID provided significantly improved BD image quality and more accurate depiction of the BD anatomy and BD openings at right donor hemihepatectomy than 3D-T2W-MRC.

Key Words: isotropic high-resolution, iterative denoising algorithm, T1W, magnetic resonance cholangiography, 60-channel coil, living donor liver transplantation, bile duct

(*Invest Radiol* 2019;54: 103–109)

Received for publication June 11, 2018; and accepted for publication, after revision, August 18, 2018.

From the *Department of Radiology, Seoul National University Hospital; †Department of Radiology, Seoul National University College of Medicine, Seoul; ‡Department of Radiology, Gachon University Gil Medical Center, Incheon, Republic of Korea; §Siemens Healthcare GmbH, Erlangen, Germany; and ||Department of Surgery, Seoul National University Hospital, Seoul, Republic of Korea.

Conflicts of interest and sources of funding: none declare.

Correspondence to: Jeong Min Lee, MD, Department of Radiology, Seoul National University College of Medicine, 101 Daehangno, Jongno-gu, Seoul, 110-744, Republic of Korea. E-mail: jmsh@snu.ac.kr.

Copyright © 2018 Wolters Kluwer Health, Inc. All rights reserved.

ISSN: 0020-9996/19/5402-0103

DOI: 10.1097/RLI.0000000000000512

Liver transplantation has been a well-established treatment option for advanced liver cirrhosis and early-stage hepatocellular carcinoma within the Milan criteria, with a 5-year survival rate of 60% to 90%.¹ Recently, owing to the shortage of cadaveric liver donors, living donor liver transplantation (LDLT) has gained more attention as an alternative option.² However, despite continuous improvements in surgical techniques, splitting the liver remains a difficult problem, and thus more dedicated preoperative approaches using laboratory and imaging examinations are warranted for the safety of both donors and recipients. In particular, biliary complications, which are the gravest of postoperative complications, have been reported to occur more frequently in LDLT than in deceased-donor liver transplantations with an incidence of 15% to 40% in recipients^{3,4} and 4% to 13% in donors^{5,6} among all postoperative complications.^{7,8} In addition, other well-known predisposing factors of biliary complications are the number of graft bile duct (BD) openings, anatomic variation (present in 40% of the general population), and the short length of the right hepatic duct (RHD).^{9–12}

Magnetic resonance cholangiography (MRC) using 3-dimensional (3D) heavily T2-weighted (T2W) fast or turbo spin-echo sequences has been a well-established noninvasive technique for the evaluation of the BD.¹³ However, as T2W-MRCs are usually performed in a respiratory-triggered manner, its relatively long acquisition time, potentiality of severe motion artifacts related to irregular breathing, and limited signal-to-noise ratios have remain unsolved.^{14,15} In this regard, another approach to evaluating the biliary anatomy may be gadoteric acid–enhanced magnetic resonance (MR) imaging, which uses the properties of biliary excretion and the strong T1-shortening effect.^{16,17} Yet, conventional breath-hold (BH) 3D-T1W-MRC with gadoteric acid has also shown a limitation in relatively lower spatial resolution when evaluating intrahepatic bile ducts (IHDs) compared with navigator-triggered 3D-T2W-MRC with an isotropic resolution of 1 mm³, as it is usually performed with a slice thickness of 1.8 to 3 mm and an in-plane resolution of 1.3 mm to 1.5 mm.^{18,19} Thus, in an attempt to improve the limited spatial resolution of conventional T1W-MRC for biliary anatomy evaluation, navigator-triggered high-resolution (HR) T1-MRC techniques were developed providing improved image quality compared with T2W-MRC or BH-T1W-MRC.^{20–22} Yet, until now, the total scan time of navigator-triggered HR-T1W-MRC took as long as 4 to 6 minutes depending on the respiratory pattern and rate, and possessed a technical failure rate of 3.5% to 5%.^{21,23,24}

Therefore, with the use of a 60-channel phased-array coil, a 2-dimensional parallel imaging technique with a high acceleration factor, and an iterative denoising algorithm,²⁵ we endeavored to optimize the 3D-T1 gradient echo sequence for isotropic (1 mm³) HR-T1-MRC so as to be completed within 20 seconds. The purpose of this study, thus, was to evaluate the clinical feasibility of isotropic high-resolution (IHR) 3D-T1W-MRC using iterative denoising in comparison with conventional 3D-T2W-MRC for evaluation of the biliary anatomy of living liver donors.

MATERIALS AND METHODS

This study was approved by our institutional review board, and the requirement for informed consent was waived owing to its retrospective nature. The prototype implementation of 3D VIBE Dixon acquisition and reconstruction was provided by Siemens Healthcare and an employee of Siemens Healthcare (K.S.) provided technical support for software implementation. However, authors not associated with Siemens Healthcare (H.J.K. and J.M.L.) maintained full control of the data at all times.

Patients

From April 2015 through March 2017, 140 potential living liver donor candidates of suitable medicopsychological status who were willing to donate their liver underwent MR imaging. A flow diagram of the patient population is described in Figure 1. Among them, 41 potential donors did not undergo hepatectomy owing to recipient ($n = 23$) or donor factors ($n = 18$). In addition, 24 donors were further excluded from analysis as they had undergone left hepatectomy ($n = 6$) and had no IHR-T1W-MRC images ($n = 18$). Finally, a total of 75 patients (mean age, 35.2 years; range, 17–60 years), including 48 men (mean age, 32.9 years; range, 17–60 years) and 27 women (mean age, 40.1 years; range, 19–57 years), underwent right hepatectomy for liver donation (open hepatectomy, $n = 33$; laparoscopic hepatectomy, $n = 42$), comprising our study population.

MR Image Acquisition

All images were obtained using a 3 T MR scanner (MAGNETOM Skyra; Siemens Healthcare, Erlangen, Germany) with a torso 60-channel phased-array coil.

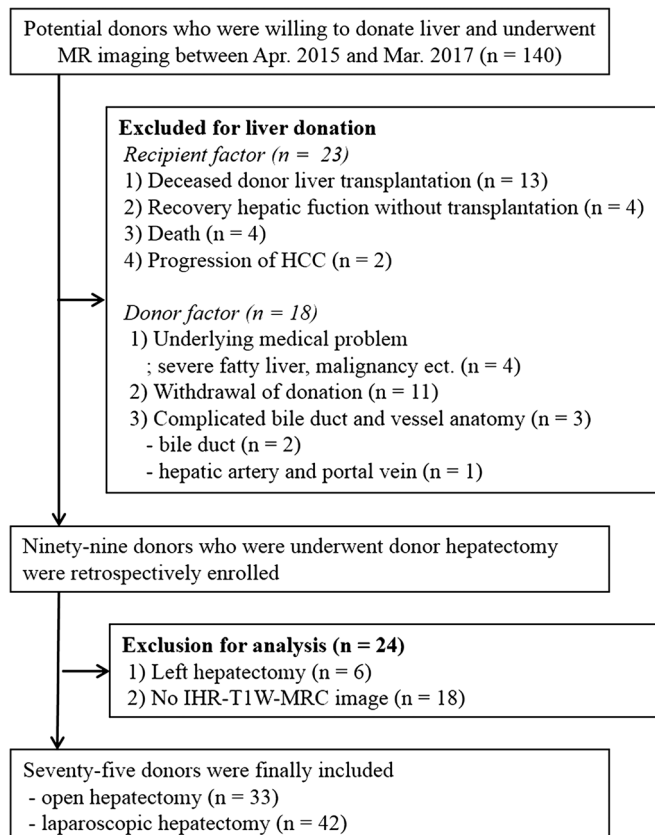


FIGURE 1. Flow diagram of patients' population.

T2-Weighted Magnetic Resonance Cholangiography

Three-dimensional T2W-MRC was performed via a respiratory-triggered multisection 3-dimensional (3D) turbo spin-echo sequence (field of view [FOV], $256 \times 256 \text{ mm}^2$; matrix 256×256 ; repetition time [TR] variable depending on respiratory rate; echo time [TE], 661 milliseconds; flip angle [FA], 100 degrees; section thickness [ST], 1 mm; resolution, $1 \times 1 \times 1 \text{ mm}^3$; 80–96 slices; acquisition time varying with the breathing pattern of patient). Three-dimensional T2W-MRC data were reconstructed using a maximum intensity projection algorithm provided at the MR console.

Isotropic High-Resolution T1W-MRC

For IHR-T1W-MRC with a small FOV ($256 \times 256 \text{ mm}^2$, $1 \times 1 \times 1 \text{ mm}^3$ resolution), BH fat-suppressed 3D spoiled gradient echo Dixon sequences (CAIPRHINA VIBE Dixon; Siemens Healthcare, Erlangen, Germany) and a retro-reconstruction iterative denoising algorithm were used.

A prototype iterative denoising algorithm, which consists of an inner core of multiwavelet thresholding as a regularizer, was integrated into the scanner reconstruction pipeline.²⁶ During the iterations, the current regularized image was optimally combined with the original image and the previous image estimate, according to Stein's unbiased risk estimator.²⁷ The algorithm then worked on complex-valued 3D volumes (after channel combination), taking into account both the spatially varying noise level in the image, the g-factor from parallel imaging, and k-space filter functions. Noise in the raw data was measured via a prescan by the system and was used as a quantitative input. The algorithm thus adapted automatically to changes in acquisition and reconstruction settings, as well as to changes in scan conditions.

High-resolution T1W-MRCs were obtained in the axial and coronal planes 20 minutes after gadoxetic acid (Primovist or Eovist; Bayer Healthcare, Berlin, Germany) injection at a standard dose of 0.1 mL/kg body weight. Detailed acquisition parameters are as follows: FOV, $256 \times 208 \text{ mm}^2$; matrix, 256×208 ; TR, 6.3 milliseconds; TE, 2.5 milliseconds; FA, 30 degrees; ST, redundant with 3D resolution; resolution, $1 \times 1 \times 1 \text{ mm}^3$; 128 slices; acceleration factor, 2×2 ; and a 3D pattern shift 1 in axial T1W-MRC scans. In addition, for coronal T1W-MRC, FOV, $256 \times 256 \text{ mm}^2$; matrix, 256×256 ; TR, 6.2 milliseconds; TE, 2.5 milliseconds; FA, 30 degrees; ST, redundant with 3D resolution; resolution, $1 \times 1 \times 1 \text{ mm}^3$; 88 slices; acceleration factor, 4; and phase oversampling of 26% were used.

Image Analysis

Three board-certified radiologists (S.J.A., H.J.K., and J.S.B. with 9, 7, and 6 years of clinical experience in abdominal MR imaging, respectively) independently reviewed the conventional 3D-T2W-MRC and IHR-T1W-MRC examinations with at least a 2-week interval to minimize recall bias. All images were anonymized, and the reviewers were blinded to the surgical findings of biliary trees and the results of the BD opening number at right donor hepatectomy.

Image Quality Analysis

Bile duct visibility and image blurring (sharpness) were evaluated on a 5-point scale for the common bile duct (CBD) and bilateral first and second IHDs. Overall image quality was also assessed on a 5-point scale with the highest score indicating better image quality. Detailed description of each score is noted in Table 1.

Diagnostic Performance Analysis

The reviewers were requested to determine the anatomy types of BDs according to the 5 anatomy types reported by Huang et al,²⁸ that is, normal, trifurcation, right posterior BD draining to the left hepatic duct, right posterior BD draining to the common BD, and right posterior BD

TABLE 1. Scoring Scale of Various Parameters in the Assessment of Image Quality and Confidence Levels for Each MRC

Parameter	Score	Scoring System
Overall image quality	1–5	Score 1, uninterpretable; 2, poor (below average); 3, fair (average); 4, good (above average); 5, excellent
Image blurring	1–5	Score 1, nondiagnostic (hampering diagnostic capability); 2, extremely blurred (not hampering diagnostic capability but significantly decreased image quality); 3, moderate blurring (moderate image quality degradation); 4, mild blurring; (mild image quality degradation); 5, no blurring
Duct visualization	1–5	Score 1, nonvisualization; 2, poorly visualized with limited diagnostic value; 3, partially visualized; 4, near complete visualization; 5, excellent clear visualization
Confidence level for determining BD opening number	1–4	Score 1, nonconfident (<50% confidence); 2, mildly confident (50%~70%); 3, moderately confidence (71%~90%); 4, highly confident (>90%)

draining to the cystic duct. Normal BD anatomy was defined as the right posterior BD draining to the RHD, with the right and left hepatic ducts joining the common hepatic duct.²⁹ In addition, the measured length of the RHD and expected number of BD openings at right hepatectomy were recorded along with their confidence level on a 4-point scale in determining the number of BD openings (Table 1).

Intraoperative Correlation

All 75 donors underwent right hepatectomy performed by 3 surgeons (K.S.S., K.W.L., and N.J.L. with 27, 20, and 17 years of experience in liver transplantation and hepatectomy, respectively) in the

same institute. During the operation, real-time fluorescent cholangiography was obtained 30 to 60 minutes after intravenous injection of indocyanine green (0.05 mg/kg) with either LuxEndoBright (Korea Electrotechnology Research Institute, Seoul, South Korea) or Pinpoint (Novadaq, Ontario, Canada).³⁰ After the bilateral first and second BD branches were clearly visualized, they carefully compared the results of real-time fluorescent cholangiography with preoperative MRC imaging. The appropriate cutting lines of the donor's BDs were determined by the surgeon based on real-time fluorescent cholangiography and MRC images. They recorded the hilar branching anatomy of the BD, the number of BD openings along the surgical resection plane of right

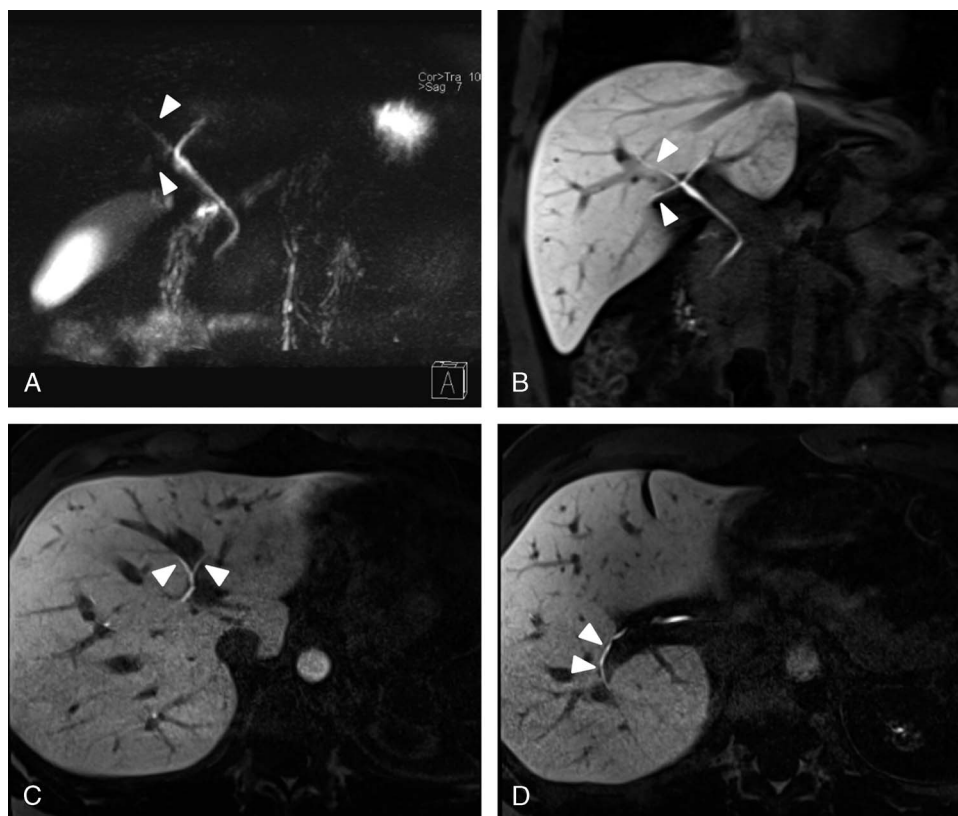


FIGURE 2. Magnetic resonance cholangiography (MRC) images of a 23-year-old man. On conventional 3D-T2W-MRC (A), right second intrahepatic ducts (IHD) are blurred and limited to evaluate BD anatomy (arrowheads), whereas IHR-T1W-MRC (B) shows right second IHD clearly (arrowheads) with pronounce BD variation of trifurcation into the left hepatic duct and the right anterior and posterior bile duct. Axial images of IHR-T1W-MRC also depict left (C, arrowheads) and right (D, arrowheads) second IHDs clearly.

hepatectomy, and the number of BD anastomosis. The intraoperative record was then compared with the MRC findings.

Statistical Analysis

Continuous variables were expressed as means \pm standard deviation and BD visibility, image blurring, overall image quality, and confidence level of the number of BD openings on right hepatectomy were analyzed using the paired *t* test with commercially available statistical software (SPSS version 22; IBM Corporation, Armonk, NY). A *P* value of less than 0.05 was considered to indicate a statistically significant difference. In addition, the McNemar test was used to evaluate the consistency of the expected number of BD openings and anatomic variation using the same software. Interobserver agreements for RHD length were analyzed using another commercially available statistical software program (Medcalc, version 16.4, MedCalc Software, Ostend, Belgium). The strength of agreement was evaluated as follows: an ICC value of less than 0.20 indicated poor agreement; 0.21–0.40, fair agreement; 0.41–0.60, moderate agreement; 0.61–0.80, good agreement; and 0.81–1.0, excellent agreement.

RESULTS

The mean acquisition times of 3D-T2W-MRC and IHR-T1W-MRC were 367 ± 96 seconds and 17 ± 2 seconds, respectively ($P < 0.001$).

Overall Image Quality

Isotropic high-resolution T1W-MRC demonstrated significantly better overall image quality (4.24 ± 0.79 vs 3.59 ± 1.09 , $P < 0.001$) than

3D-T2W-MRC. The number of uninterpretable or poor image quality (score ≤ 2) scans were significantly decreased with IHR-T1W-MRC compared with 3D-T2W-MRC (2.2% [5/225] vs 17.8% [40/225], $P < 0.01$). Representative examples are presented in Figures 2 and 3.

Duct Visualization

Bilateral first- and second-order IHDs were better visualized on IHR-T1W-MRC with less image blurring compared with 3D-T2W-MRC (All *P*s < 0.05). Differences in visibility were more pronounced in the second-order IHDs than proximal BDs (Table 2). As for the CBD, IHR-T1W-MRC did not present better visibility than 3D-T2W-MRC (4.50 ± 0.68 vs 4.51 ± 0.80 , $P = 0.83$), but showed less image blurring (4.59 ± 0.69 vs 4.24 ± 0.82 , $P < 0.001$).

Diagnostic Performance Analysis

On IHR-T1W-MRC, the number of noninterpretable scans for evaluation of the biliary anatomy were significantly decreased compared with 3D-T2W-MRC (0.4% [1/225] vs 4.0% [9/225], $P = 0.02$). More specifically, only one noninterpretable case was noted by reviewer 1 in IHR-T1W-MRC, whereas 5, 1, and 3 cases were noted with 3D-T2W-MRC for each reviewer, respectively. Indeed, IHR-T1W-MRC showed higher agreement with the reference standard using a combination of intraoperative indocyanine green real-time fluorescent cholangiography results and surgical findings in biliary anatomy evaluation than 3D-T2W-MRC (87.6% [197/225] vs 81.3% [183/225], $P = 0.03$, Table 3). Representative examples are presented in Figures 2 and 3.

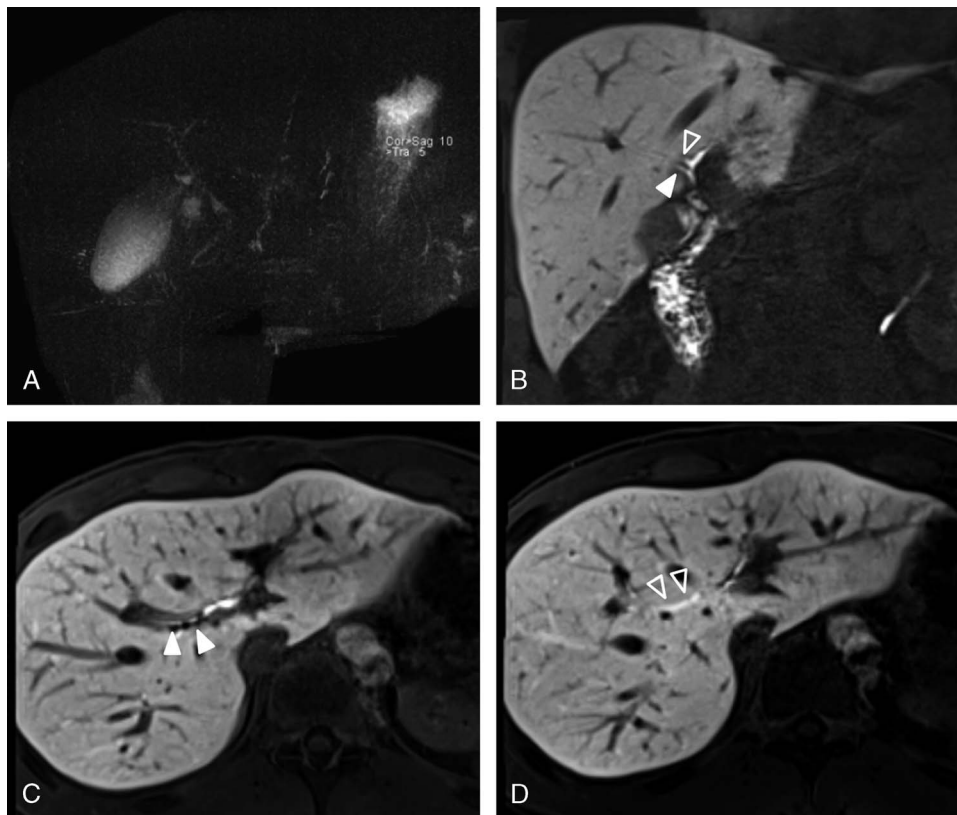


FIGURE 3. Magnetic resonance cholangiography (MRC) images of a 29-year-old man. On conventional 3D-T2W-MRC (A), overall image quality is poor and limited to evaluate BD anatomy and BD opening number. However, IHR-T1W-MRC (B) shows right anterior (white arrowhead) and posterior BD (empty arrowhead) clearly, with BD variation that is right posterior BD draining the left hepatic duct. Axial images of IHR-T1W-MRC also depict right anterior (C, white arrowheads) and posterior (D, empty arrowheads) BD clearly. Two of 3 reviewers interpreted BD anatomy as normal in conventional 3D-T2W-MRC, whereas all 3 reviewers showed consistency with reference standard to interpret BD variation and BD opening number in IHR-T1W-MRC. On operation records, there were 2 BD openings in graft resection margin.

TABLE 2. Comparison of Image Quality Between 3D-T2W-MRC and IHR-T1W-MRC

		Duct Visualization			P
		3D-T2W-MRC	IHR-T1W-MRC	Mean Difference	
Duct visualization	CBD	4.51 ± 0.80	4.50 ± 0.68	0.01	0.83
	Right first IHD	3.92 ± 1.30	4.28 ± 1.30	0.36	<0.001
	Left first IHD	4.31 ± 0.90	4.65 ± 0.62	0.34	<0.001
	Right second IHD	3.42 ± 1.06	4.23 ± 0.82	0.81	<0.001
	Left second IHD	3.25 ± 1.04	3.97 ± 0.93	0.72	<0.001
Image blurring	CBD	4.59 ± 0.69	4.24 ± 0.82	0.35	<0.001
	Right first IHD	3.62 ± 1.32	4.17 ± 1.27	0.56	<0.001
	Left first IHD	4.02 ± 1.01	4.50 ± 0.70	0.48	<0.001
	Right second IHD	3.27 ± 1.10	4.08 ± 0.79	0.81	<0.001
	Left second IHD	3.01 ± 1.10	3.81 ± 0.88	0.80	<0.001

Data are mean values ± standard deviations.

3D indicates 3-dimensional; T2W, T2-weighted; MRC, magnetic resonance cholangiography; IHR, isotropic high-resolution; T1W, T1-weighted; IHD, intrahepatic bile duct; CBD, common bile duct.

Regarding the number of BD openings on right hepatectomy, IHR-T1W-MRC presented significantly higher agreement with the reference standard than 3D-T2W-MRC (76.9% [173/225] vs 70.2% [158/225], $P = 0.006$, Table 4) with a higher confidence score (3.62 ± 0.64 vs 3.23 ± 0.89 , $P < 0.001$).

The mean RHD lengths were 5.80 ± 5.3 mm, 5.64 ± 5.4 mm, and 6.11 ± 6.3 mm on 3D-T2W-MRC, and 6.10 ± 5.7 mm, 5.7 ± 6.1 mm, and 5.69 ± 5.2 mm on IHR-T1W-MRC estimation of each reviewer. There were no statistical significances between MRCs in RHD length in all reviewers. However, IHR-T1W-MRC showed excellent interobserver agreement (ICC, 0.94; range, 0.91–0.96), whereas 3D-T2W-MRC showed good interobserver agreement (ICC, 0.78; range, 0.67–0.86).

DISCUSSION

Our study demonstrated that IHR-T1W-MRC using iterative denoising provides better image quality and diagnostic performance than conventional 3D-T2W-MRC for the evaluation of the biliary anatomy of living liver donors. Specifically, IHR-T1W-MRC showed higher agreement with the reference standard in revealing the biliary anatomy and the number of BD openings in liver donor grafts. We can attribute this improvement in diagnostic performance to the significantly superior overall image quality and visibility of bilateral first- and second-order IHDs with less image blurring using IHR-T1W-MRC. Indeed, a precise preoperative definition of the BD anatomy of liver donor candidates, especially in hilar confidence level, is crucial in determining their candidacy for liver donation and in surgical planning.¹¹ For instance, in our study, 2 donor candidates (1.4%) were rejected for liver donation owing to complex BD anatomy. Thus, considering that segmental intrahepatic ducts in liver donor candidates are not dilated and are usually 0.5 to 1.5 mm in diameter, higher spatial resolution MRC is strongly warranted for biliary evaluation of potential donors.

In our study, IHR-T1W-MRC was able to provide 1 mm^3 isotropic spatial resolution for evaluation of small biliary ductal anatomy. In general, conventional BH-T1W-MRCs show limited spatial resolution compared with 3D-T2W-MRC for the evaluation of IHDs, as those sequences are usually acquired with a slice thickness of 2 to 3 mm and an in-plane resolution of 1.3 to 1.5 mm. Yet, the most pronounced obstacles for the higher spatial resolution of conventional T1W-MRC is the time limitation, as it is performed in BH, as well as its higher noise and the low signal of the organ at interest. Although respiratory-triggered T1W-MRC may provide spatial resolution comparable with 3D-T2W-MRC, it would be affected by irregular breathing and would require even longer acquisition time.²³ Thus, our results using IHR-T1W-MRC with

iterative denoising hold clinical importance. There were several contributing factors for the high spatial resolution of our IHR-T1W-MRC while maintaining good SNR, including the use of a 60-channel phased-array coil, an effective 2-dimensional parallel imaging technique, and an iterative noise reduction algorithm. Further studies are warranted to determine which combination of factors would best provide the highest spatial resolution in future studies.

It would also be possible to obtain high spatial resolution images using conventional 3D-T2W-MRC; however, it would be accompanied by a relatively long acquisition time and motion artifacts arising from irregular breath rhythms as it would be performed in a respiratory triggered manner, resulting in image quality degradation. Likewise, in our study, we found significantly more uninterpretable or poor image quality cases with 3D-T2W-MRC than with IHR-T1W-MRC, while consuming substantially longer acquisition time (367 seconds vs 17 seconds, $P < 0.001$). With recent developments in MR technology, however, BH-T2W-MRC are now possible using compressed sensing via high k-space undersampling^{14,31} or fast data acquisition techniques such as gradient and spin-echo,^{32,33} 3D balanced steady-state free precession, or fast-recovery fast spin-echo sequences.³⁴ However, those sequences have failed to show consistent clinically acceptable image quality compared with conventional respiratory triggered T2W-MRC, owing to requirements of higher performance hardware and software for compressed sensing, vulnerability to artifacts related to the echo-planar component of the gradient and spin-echo technique, and banding artifacts using balanced steady-state free precession methods.^{32,33} Therefore, we suggest that IHR-T1W-MRC could be used as a good alternative that can present better image quality, short acquisition time, and high spatial resolution for the evaluation of BD.

TABLE 3. Agreements in Biliary Anatomy Evaluation Between MRCs and the Reference Standard

	Reviewer 1	Reviewer 2	Reviewer 3	Total
3D-T2W-MRC	55/75 (73.3)	70/75 (93.3)	58/75 (77.3)	183/225 (81.3)
IHR-T1W-MRC	64/75 (85.3)	72/75 (96.0)	65/75 (86.7)	201/225 (89.3)
P	0.04	0.50	0.12	0.03

Numbers in parentheses are percentages.

3D indicates 3-dimensional; T2W, T2-weighted; MRC, MR cholangiography; IHR, isotropic high-resolution; T1W, T1-weighted.

TABLE 4. Agreements in the Number of BD Openings Between MRC-Based Expectations and the Reference Standard

	Reviewer 1	Reviewer 2	Reviewer 3	Total	Confidence Score
3D-T2W-MRC	50/75 (66.7)	60/75 (80.0)	48/75 (64.0)	158/225 (70.2)	3.23 ± 0.89
IHR-T1W-MRC	58/75 (77.3)	64/75 (85.3)	51/75 (68.0)	173/225 (76.9)	3.62 ± 0.64
P	0.02	0.22	0.55	0.006	<0.001

Numbers in parentheses are percentages.

3D indicates 3-dimensional; T2W, T2-weighted; MRC, MR cholangiography; IHR, isotropic high-resolution; T1W, T1-weighted.

Finally, in our study, IHR-T1W-MRC demonstrated excellent interobserver agreement in estimating the length of the RHD, whereas 3D-T2W-MRC only showed good interobserver agreement (ICC values, 0.94, 0.78, respectively) among the 3 reviewers. Consistent and reproducible BD measurement is essential for surgical planning as a short RHD of the donor may result in a higher chance of multiple BD openings and biliary complications than a long RHD.^{10,35} In this regard, higher interobserver agreement in estimating the length of BD using IHR-T1W-MRC are noteworthy.

There are several study limitations that we should acknowledge. First, due to the retrospective nature of this study, selection bias was not avoidable. Second, our study was done on a single-center basis, and our study population was relatively small, thereby limiting the generalization of our study results. Third, as we had excluded donors who underwent left hepatectomy for study population uniformity, our results may not be extrapolated to all cases of LDLT. Nevertheless, the focus of the current study was the evaluation of BD anatomy. Thus, the difference in surgical technique might only have a minimal influence.

In conclusion, IHR-T1W-MRC with iterative denoising provided significantly improved image quality, BD sharpness, and higher interobserver agreement in RHD length measurement, resulting in more accurate expectation of BD anatomy and number of BD openings in right donor hepatectomy than 3D-T2W-MRC, which is crucial for the prevention of postoperative biliary complications of living liver transplantation.

ACKNOWLEDGMENTS

We thank to Chris Woo (B.A., United States) for his editorial assistance.

REFERENCES

- Befeler AS, Hayashi PH, Di Bisceglie AM. Liver transplantation for hepatocellular carcinoma. *Gastroenterology*. 2005;128:1752–1764.
- Kulik L, Abecassis M. Living donor liver transplantation for hepatocellular carcinoma. *Gastroenterology*. 2004;127(5 Suppl 1):S277–S282.
- Brown RS Jr, Russo MW, Lai M, et al. A survey of liver transplantation from living adult donors in the United States. *New Engl J Med*. 2003;348:818–825.
- Broering DC, Sterneck M, Rogiers X. Living donor liver transplantation. *J Hepatol*. 2003;38:119–135.
- Brown S Jr, Richardson M, Lai M. Adult living donor liver transplantation (LDLT) in the US: results of a survey from the NIH LDLT Meeting. *Hepatology*. 2001;34(4 Pt 2):235A.
- Fujita S, Kim ID, Uryuhara K, et al. Hepatic grafts from live donors: donor morbidity for 470 cases of live donation. *Transpl Int*. 2000;13:333–339.
- Welling TH, Heidt DG, Englesbe MJ, et al. Biliary complications following liver transplantation in the model for end-stage liver disease era: effect of donor, recipient, and technical factors. *Liver Transplant*. 2008;14:73–80.
- Wadhawan M, Kumar A, Gupta S, et al. Post-transplant biliary complications: an analysis from a predominantly living donor liver transplant center. *J Gastroenterol Hepatol*. 2013;28:1056–1060.
- Kashyap R, Bozorgzadeh A, Abt P, et al. Stratifying risk of biliary complications in adult living donor liver transplantation by magnetic resonance cholangiography. *Transplantation*. 2008;85:1569–1572.
- Jeon YM, Lee KW, Yi NJ, et al. The right posterior bile duct anatomy of the donor is important in biliary complications of the recipients after living-donor liver transplantation. *Ann Surg*. 2013;257:702–707.

- Ragab A, Lopez-Soler RI, Oto A, et al. Correlation between 3D-MRCP and intraoperative findings in right liver donors. *Hepatobiliary Surg Nutr*. 2013;2:7.
- Low G, Wiebe E, Walji AH, et al. Imaging evaluation of potential donors in living-donor liver transplantation. *Clin Radiol*. 2008;63:136–145.
- Xu YB, Bai YL, Min ZG, et al. Magnetic resonance cholangiography in assessing biliary anatomy in living donors: a meta-analysis. *World J Gastroenterol*. 2013;19:8427–8434.
- Yoon JH, Lee SM, Kang HJ, et al. Clinical feasibility of 3-dimensional magnetic resonance cholangiopancreatography using compressed sensing: comparison of image quality and diagnostic performance. *Invest Radiol*. 2017;52:612–619.
- Kang HJ, Lee JM, Yoon JH, et al. Additional values of high-resolution gadoxetic acid-enhanced MR cholangiography for evaluating the biliary anatomy of living liver donors: comparison with T₂-weighted MR cholangiography and conventional gadoxetic acid-enhanced MR cholangiography. *J Magn Reson Imaging*. 2018;47:152–159.
- Lee NK, Kim S, Lee JW, et al. Biliary MR imaging with Gd-EOB-DTPA and its clinical applications. *Radiographics*. 2009;29:1707–1724.
- Kinner S, Steinweg V, Maderwald S, et al. Bile duct evaluation of potential living liver donors with Gd-EOB-DTPA enhanced MR cholangiography: single-dose, double dose or half-dose contrast enhanced imaging. *Eur J Radiol*. 2014;83:763–767.
- Choi JY, Lee JM, Lee JY, et al. Navigator-triggered isotropic three-dimensional magnetic resonance cholangiopancreatography in the diagnosis of malignant biliary obstructions: comparison with direct cholangiography. *J Magn Reson Imaging*. 2008;27:94–101.
- Cai L, Yeh BM, Westphalen AC, et al. 3D T₂-weighted and Gd-EOB-DTPA-enhanced 3D T₁-weighted MR cholangiography for evaluation of biliary anatomy in living liver donors. *Abdom Radiol (NY)*. 2017;42:842–850.
- Kinner S, Schubert TB, Said A, et al. Added value of gadoxetic acid-enhanced T₁-weighted magnetic resonance cholangiography for the diagnosis of post-transplant biliary complications. *Eur Radiol*. 2017;27:4415–4425.
- Frydrychowicz A, Jedynak AR, Kelcz F, et al. Gadoxetic acid-enhanced T₁-weighted MR cholangiography in primary sclerosing cholangitis. *J Magn Reson Imaging*. 2012;36:632–640.
- Lee JH, Kim B, Kim HJ, et al. High spatial resolution navigated 3D T₁-weighted hepatobiliary MR cholangiography using Gd-EOB-DTPA for evaluation of biliary anatomy in living liver donors. *Abdom Radiol (NY)*. 2018.
- Lee ES, Lee JM, Yu MH, et al. High spatial resolution, respiratory-gated, T₁-weighted magnetic resonance imaging of the liver and the biliary tract during the hepatobiliary phase of gadoxetic acid-enhanced magnetic resonance imaging. *J Comput Assist Tomogr*. 2014;38:360–366.
- Yoon JH, Lee JM, Lee ES, et al. Navigated three-dimensional T₁-weighted gradient-echo sequence for gadoxetic acid liver magnetic resonance imaging in patients with limited breath-holding capacity. *Abdom Imaging*. 2015;40:278–288.
- Kannengiesser SA, Mailhe B, Nadar M, et al. Universal iterative denoising of complex-valued volumetric MR image data using supplementary information. *ISMRM*. 2016. Available at: <http://indexsmart.mirasart.com/ISMRM2016/PDFfiles/1779.html>.
- Luisier F, Blu T, Unser M. SURE-LET for orthonormal wavelet-domain video denoising. *IEEE Transactions on Circuits and Systems for Video Technology*. 2010;20:913–919.
- Blu T, Luisier F. The SURE-LET approach to image denoising. *IEEE Trans Image Process*. 2007;16:2778–2786.
- Huang TL, Cheng YF, Chen CL, et al. Variants of the bile ducts: clinical application in the potential donor of living-related hepatic transplantation. *Transplant Proc*. 1996;28:1669–1670.
- Catalano OA, Singh AH, Uppot RN, et al. Vascular and biliary variants in the liver: implications for liver surgery. *Radiographics*. 2008;28:359–378.
- Hong SK, Lee KW, Kim HS, et al. Optimal bile duct division using real-time indocyanine green near-infrared fluorescence cholangiography during laparoscopic donor hepatectomy. *Liver Transplant*. 2017;23:847–852.

31. Chandarana H, Doshi AM, Shanbhogue A, et al. Three-dimensional MR cholangiopancreatography in a breath hold with sparsity-based reconstruction of highly undersampled data. *Radiology*. 2016;280:585–594.
32. Wielopolski PA, Gaa J, Wielopolski DR, et al. Breath-hold MR cholangiopancreatography with three-dimensional, segmented, echo-planar imaging and volume rendering. *Radiology*. 1999;210:247–252.
33. Nam JG, Lee JM, Kang HJ, et al. GRASE Revisited: breath-hold three-dimensional (3D) magnetic resonance cholangiopancreatography using a Gradient and Spin Echo (GRASE) technique at 3T. *Eur Radiol*. 2018;28:3721–3728.
34. Sodickson A, Mortelet KJ, Barish MA, et al. Three-dimensional fast-recovery fast spin-echo MRCP: comparison with two-dimensional single-shot fast spin-echo techniques. *Radiology*. 2006;238:549–559.
35. Ishiko T, Egawa H, Kasahara M, et al. Duct-to-duct biliary reconstruction in living donor liver transplantation utilizing right lobe graft. *Ann Surg*. 2002;236:235.